Binary SbTe Phase Diagrams developed by Material Library Technique

Ting Zhang[1,2], Zhitang Song[1], Bo Liu[1], Yifeng Gu[1], Songlin Feng[1], Martin Salinga[2], and Matthias Wuttig[2]
[1]State Key Laboratory of Functional Materials for Informatics, Laboratory of Nanotechnology, Shanghai Institute of Microsystem and Information Technology, Chinese Academy of Sciences, 200050 Shanghai, China
[2]Institute of Physics (IA), RWTH Aachen University, 52056 Aachen, Germany
T. Zhang email: tzhang@mail.sim.ac.cn

ABSTRACT

New binary SbTe phase diagrams with phase change information were developed by means of material library technique. Compositional gradient Sb_xTe_{1-x} ($0 \le x \le 1$) film was prepared and characterized by far-field optical testing. Phase change parameters such as switching power and speed were illustrated in the phase diagrams. Promising compositions for memory applications were proposed based on the phase diagrams. The phase diagrams show that compositions around x=0.4 possess a high programming speed and a low switching power, but a poor thermal stability. When x is in the range from 0.5 to 0.72, both programming speed and switching power are outstanding. What is more important, the data retention for these compositions is much better than Sb_2Te_3. Hence subsequently phase change random access memory cells based on Sb_2Te were fabricated and characterized.

Key words: phase diagram, phase change material, Sb-Te, material library technique, phase change memory.

1. INTRODUCTION

Low power consumption, high speed and high data retention are desired qualities for phase change random access memories which are presently considered as one of the most promising candidates for the next-generation non-volatile semiconductor memory applications. Since the performance of these devices is basically determined by the properties of phase change storage media, in recent years, great efforts have been made to develop novel high performance phase change materials. Various kinds of phase change materials, which have advantages of low power consumption and high speed, have been developed and studied.[1] Among those traditional phase change materials, Sb-Te has been frequently studied. Binary Sb-Te alloys have not only been investigated for the potential in optical disks but also for the applications in electronic memories.[2,3] However, no systematic study on the properties of Sb_xTe_{1-x} with Sb content range from 0 to 100 at.% has been reported.[4,5] On the other hand, phase diagrams play an important role in material science. Traditional phase diagrams provide information like the melting temperature, structure, phase transition and so on. Although the binary Sb-Te phase diagram has been measured[6] no information related to programming power and speed is included. However, this information is important for both the phase change material research and the PCRAM application. Therefore, a new phase diagram with parameters of the memory switching would be significant for its research and applications. In this work, material library (material chip) technique, a powerful technique for new materials research and development, was employed to develop an extended phase diagrams of Sb-Te. Sb_xTe_{1-x} films with a compositional gradient in the range of $0 \le x \le 1$ have been prepared applying this technique. The switching properties of the resulting materials were studied by means of far-field optical testing. From those data diagrams were developed which related composition and properties. These new Sb-Te composition diagrams are a good addition to the traditional one as shown in Figure 1. Based on the evaluation of the diagrams, promising Sb-Te compositions can be identified and proposed for memory applications. PCRAM cells based on a selected composition have been fabricated and characterized by electrical testing as well.

2. EXPERIMENTS

To develop new phase diagrams of Sb-Te, a film with a compositional gradient in the range of Sb_xTe_{1-x} ($0 \le x \le 1$) was prepared on a SiO_2/Si substrate by means of material library technique. The schematic cross-section of the film is shown in Figure 2. The Sb_xTe_{1-x} film is sandwiched between two SiO_2 layers. The thicknesses for the top and the

bottom SiO_2 capping layers are 15 and 50 nm, respectively. Eight periods of Sb/Te stacks have been deposited by sputtering to prepare the compositional gradient film. In a single period, from left to right (in Figure 1), the thickness of the Sb layers increases linearly from 0 nm to 5.8 nm, while that of the Te layers decreases linearly from 6.2 to 0 nm. The length of the compositional gradient Sb_xTe_{1-x} sample is 2.5 cm.

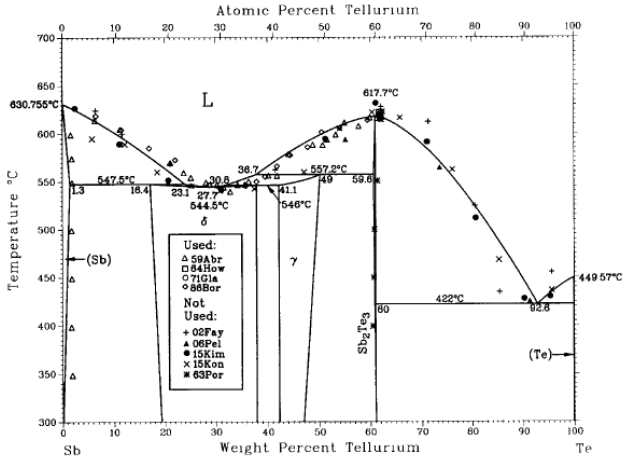

Figure 1: Calculated Sb-Te phase diagram along with experimental data.[7]

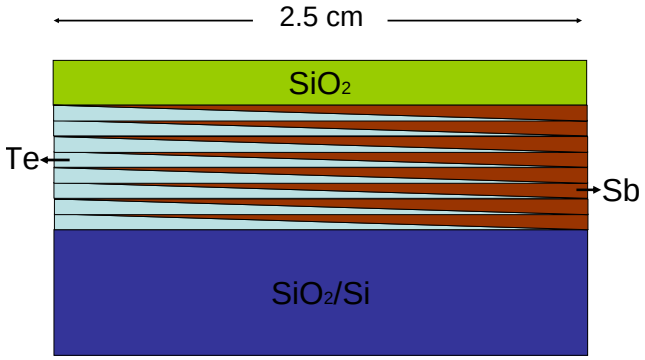

Figure 2: Schematic cross-section for the compositional gradient Sb_xTe_{1-x}. Eight periods of Sb/Te layers have been prepared to achieve the film.

The Sb_xTe_{1-x} ($0 \le x \le 1$) material chip was characterized by far-field optical testing applying a laser with a wavelength of 830 nm. In the optical testing setup, a laser pulse with a power up to 33 mW and a width as short as 10 ns could be achieved. A low power probe pulse was employed to determine the local reflectance before and after the irradiation with laser pulses. A power-time-effect (PTE) diagram, presenting the relative reflectivity change of the phase change film upon laser irradiation as a function of pulse width and power, is achieved by these experiments. The typical optical testing procedure for a composition is shown below: (1) Crystallization process. Optical reflectivity versus laser pulse duration and power for the as-deposited Sb_xTe_{1-x} composition was recorded in this step. Due to the heating effect of a laser pulse, the as-deposited bits would change to the polycrystalline state if an appropriate laser pulseis applied, accompanied by an increase of optical reflectivity. The pulse, which resulted in the highest reflectivity change (ΔR) in the PTE diagram, would be chosen as the pre-pulse in the next series of measurements. (2) Re-amorphization process. In this step, the pre-pulse obtained in the first step was applied first to transform the as-deposited Sb_xTe_{1-x} bits into a polycrystalline state. This constant pre-pulse was followed by a second laser pulse which was varied in power and duration. If the power of a pulse (with an appropriate width) was high enough to melt the polycrystalline bit, the bit would be re-amorphized upon melt-quenching. This re-amorphization process was accompanied by a decrease of optical reflectivity ($\Delta R<0$). By this experiment, the RESET (re-amorphization) parameters could be achieved. The pulse, with which the lowest optical reflectivity value was obtained, has been chosen as the pre-pulse for the third step of the measurement. (3) Re-crystallization process. At first, a pre-pulse was applied to re-amorphize the Sb_xTe_{1-x} films and to obtain the melt-quenched amorphous bits. Subsequently pulses of different power and duration were applied to determine the SET parameters (re-crystallization process).

In the far-field optical properties characterization, one of the purposes for the application of the pre-pulse was to SET the as-deposited Sb_xTe_{1-x} bits into crystalline state, or to RESET the region of interest into the re-amorphized state. The second goal of these pulses was the mixing of the different elements in the as-deposited sample with Sb/Te stack structure. This should help to obtain a more uniform distribution of the elements which is very important for the successful application of the material library technique. In a traditional material library study, annealing is necessary to transform the multi-layered material into a homogenous material. However, when the compositional gradient Sb_xTe_{1-x} ($0 \le x \le 1$) sample was annealed, a poor morphology was observed on the surface of the sample. This was mainly due to the serious evaporation problem of the elements within the sample. Therefore, a pre-pulse was applied to uniformly mix the material instead of annealing. Considering uniform diffusion, the thicknesses of Sb/Te stacks have been optimized to a relatively small value. To study the influence of film thickness on the properties of material, Ge-Sb-Te films with multi-layer structure have been deposited on Cu grid coated with carbon film. The thicknesses

for Ge, Sb, Te layers were 1.4, 1.9, and 5.3 nm (Ge:Sb:Te=2:2:5), respectively, which were similar with the corresponding thickness in the Sb_xTe_{1-x} material chip before-mentioned. Eight periods Ge/Sb/Te stacks were prepared as well. A bit array, corresponding to the PTE diagram, was written using laser pulses on the Ge-Sb-Te sample. Transmission electron microscopy (TEM) and selected-area electron diffraction (SAED) were then employed to study the microstructure of programmed bits on the carbon film. According to the TEM images and the SAED patterns, the as-deposited Ge-Sb-Te composition crystallizes into face-centered-cubic structure when an appropriate laser pulse was applied, which showed that the multi-layered $Ge_2Sb_2Te_5$ was similar with the homogenous $Ge_2Sb_2Te_5$ film prepared by co-sputtering method. However, no such experiments were carried out for the SbTe case.

3. RESULTS & DISCUSSION

Typical PTE diagrams achieved from the far-field optical testing for the composition of $Sb_{0.37}Te_{0.63}$ are shown in Figure 3. Figure 3(a) is the PTE diagram for the as-deposited $Sb_{0.37}Te_{0.63}$, without the application of a pre-pulse. From the result of Figure 3(a), "13.5 mW-1000 ns" were chosen as the parameters for the crystallization pre-pulse. The PTE diagram in Figure 2(b) shows the relative reflectivity change of pre-crystallized $Sb_{0.37}Te_{0.63}$, using the pre-pulse of 13.5 mW-1000 ns. "1% optical reflectivity change" was chosen as the criterion for the definition of "phase change". Based on the criterion, the RESET power and speed were determined to be 21.7 mW and 26.8 ns, respectively, from the PTE diagram shown in Figure 3(b). While the SET power and speed for the pre-amorphized bits were determined to be 5.43 mW and 27.3 ns from the PTE diagram shown in Figure 3(c). A pre-pulse of "32.9 mW-100 ns" was employed in the testing to obtain pre-amorphized bits. By repeating such experiments, phase change properties for Sb_xTe_{1-x} with various Sb content could be achieved. And finally refined binary Sb-Te phase diagrams could be developed.

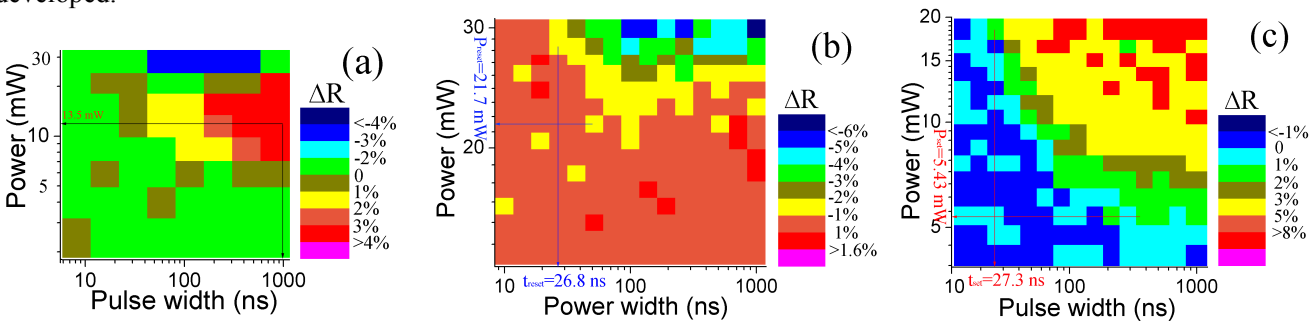

Figure 3: PTE diagrams for the composition $Sb_{0.37}Te_{0.63}$. (a) as-deposited, without pre-pulse; (b) re-crystallized, with a pre-pulse of 13.5 mW-1000 ns for pre-crystallization; (c) re-amorphized, with a pre-pulse of 32.9 mW-100 ns for pre-amorphization.

SbTe phase diagrams are shown in Figure 4. It is well known that in the applications of PCRAM and optical disk, RESET power is much higher than that of SET power and hence should be considered preferentially in the evaluation of programming power of a phase change material. RESET power phase diagram for SbTe material is shown in Figure 4(a). The phase diagram shows that composition in the x range from 0.1 to 0.45 is with a low RESET power. However, when x<0.29, the optical reflectivity changes during the SET and the RESET process were low (less than 1 %), according to the far-field testing. Te content of the composition in this range is too high, which suppresses the reversible phase change property. High content of Te should also be the reason for the low "RESET" power and high "RESET" speed (as shown in Figure 4(c)). It is well known that Te is an element with a low melting temperature and easy to evaporate. According to the traditional phase diagram, in the x range from 0.07 to 0.29, melting temperature of Sb_xTe_{1-x} decreases with increase of Te content.[7] When x=0.926, melting temperature of the composition is only about 422 °C. A low melting temperature of Sb_xTe_{1-x} with high Te content further results to a low "RESET" power and a high "RESET" speed. However, these "pre-amorphized" bits could not be changed back to crystalline state. Because of their poor reversible phase change properties, they should not be considered as reversible phase change materials. Hence, although compositions in the x range of 0.1 to 0.29 have promising "RESET" parameters, they could not be considered as a good phase change material. Consequently, the Sb_xTe_{1-x} compositions with x less than 0.29 would be excluded from the discussion below.

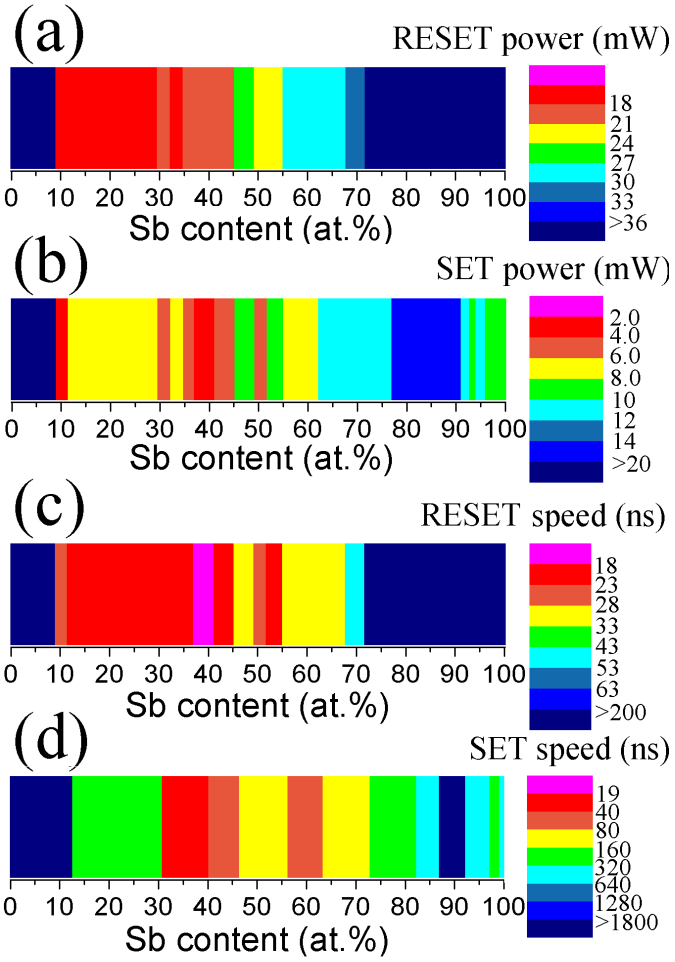

Figure 4: Binary Sb-Te phase diagrams. (a) RESET power, (b) SET power, (c) RESET speed, and (b) SET speed.

As shown in Figure 4(b) and 4(d), the composition near 0.4 is with an ultra-low SET power (less than 4 mW) and a corresponding ultra-high speed (less than 40 ns). And the RESET power and speed for the composition is about 20 mW and 18 ns, respectively. The phase diagrams show that Sb_2Te_3 (x=0.4) is a composition with a promising low power and high speed, which is already well known by the researchers in this area. On the other hand, it is also well known that the main disadvantage of Sb_2Te_3 is its low crystallization temperature. The low crystallization temperature of about 110 °C results to a poor data retention, which limits its applications in both the optical disk and the PCRAM. But the results also suggest that such phase diagrams developed using material chip technique and far-field optical testing are accurate for SbTe phase change material, without serious problems such as the problem resulted from diffusion.

Low SET power also means the amorphous state is easily to be disturbed by the environmental temperature or the light irradiation. So, considering the data retention, SET power of a phase change media should not be too low. According to the phase diagram shown in Figure 4(b), a promising candidate with better data retention is the composition with Sb content in the range from 52 at.% to 77 at.%. While according to Figure 4(d), SET speed for the composition with Sb content higher than 72 at% is relatively low (longer than 160 ns). So the composition with Sb content range from 52 at.% to 72 at.% would be more promising for the PCRAM application. In such a range, according to the phase diagrams, RESET power ranges from 21-33 mW, SET power from 4-12 mW, RESET speed from 18-53 ns, and SET speed from 40-80 ns.

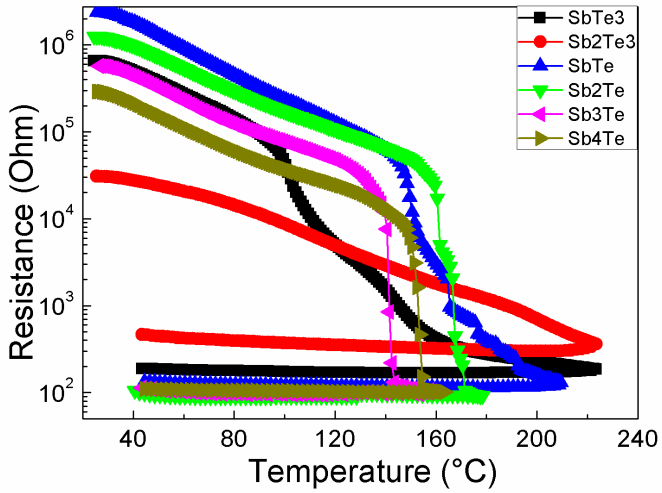

Figure 5: *In situ* temperature dependent electrical resistance for the Sb_xTe_{1-x} compositions with different Sb contents

To study the compositions in the range in detail, Sb_xTe_{1-x} with various compositions were prepared by co-sputtering and studied by means of *in situ* temperature dependent electrical resistance measurement. Resistance as a function of temperature for various Sb_xTe_{1-x} compositions is shown in Figure 5. The testing was carried out with a heating rate of 15 °C/min. According to Figure 5, when Sb content is less than 40 at.%, crystallization temperature of Sb_xTe_{1-x} is low and thermal stability is poor. However, when Sb content increases to 50 at.%, crystallization temperature increases sharply up to 150 °C, which is significantly higher than that of Sb_2Te_3. Higher crystallization temperature would result in better data retention for the application of data storage. For the composition of Sb_2Te, resistance drops quickly when temperature reaches about 160 °C. The relatively high crystallization temperature would make these binary materials promising for application of the high data retention PCRAM, for example for the automobile electronics applications.

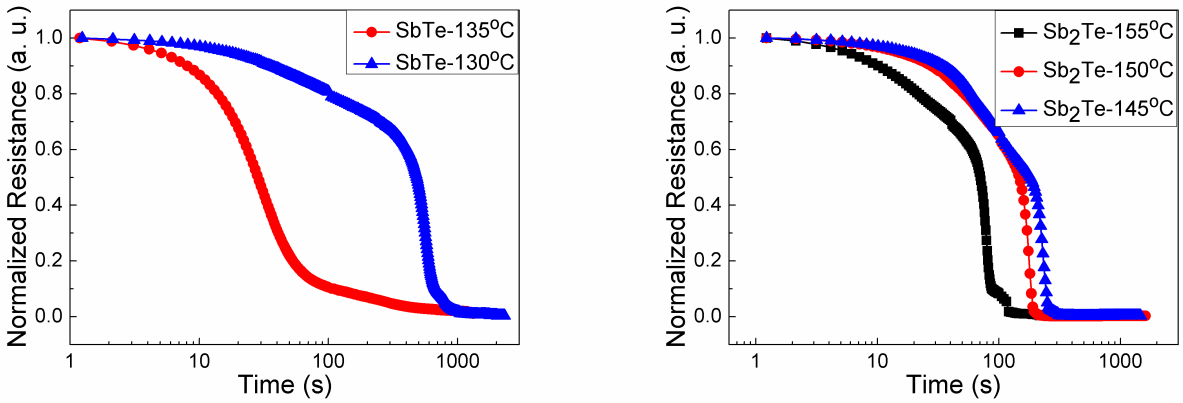

Figure 6: Normalized resistance as a function of annealing time for SbTe and Sb_2Te.

SbTe and Sb_2Te are the two typical compositions among the promising range mentioned before. Data retention for SbTe and Sb_2Te was characterized and compared. Data retention was determined by measuring time-dependent electrical resistance at a constant substrate temperature. Normalized resistance as a function of baking time for SbTe and Sb_2Te was shown in Figure 6. Sb_2Te has a better thermal stability than SbTe. According to the phase diagrams and data retention characterizations, Sb_2Te has a good programming performance and an outstanding data retention performance, which make it to be a promising candidate for the applications of PCRAM. According to the phase

diagrams, for Sb_2Te the RESET power, the SET power, the RESET speed, and the SET speed are 28 mW, 11 mW, 32 ns, and 140 ns, respectively.

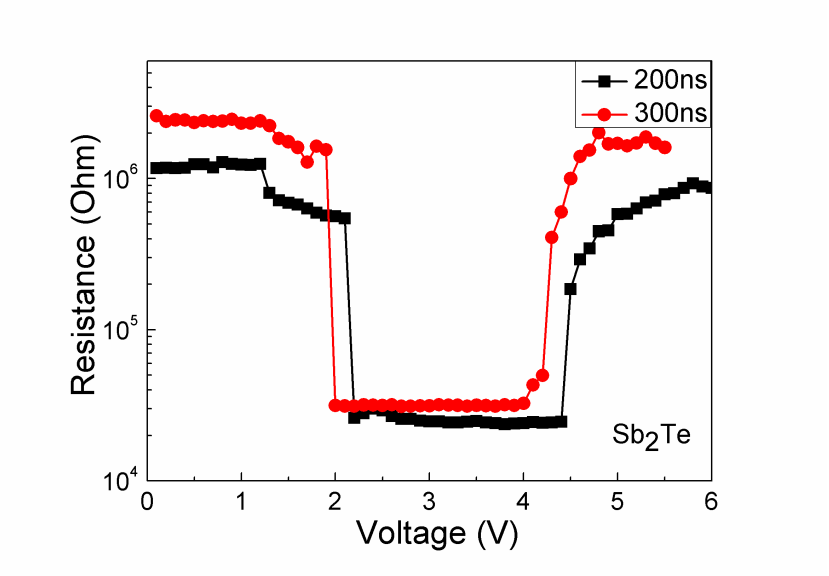

Figure 7: Typical curve for the resistance of the PCRAM cell based on Sb_2Te as a function of pulse voltage.

PCRAM device based on Sb_2Te was fabricated. The structure of the device is similar with the one elsewhere.[8] The tungsten heating electrode contact was with a diameter of 260 nm. Typical R-V curve for the device is shown in Figure 7. According to the figure, when electrical pulse with width of 200 ns was applied, PCRAM cell switches to low resistance state at 2.2 V, and switches back to high resistance state at about 5V. When the pulse width increases to 300 ns, the corresponding values drop to 1.9 V and 4.3 V, respectively. Although, the electrical performance seems to be not so outstanding as compared with $Ge_2Sb_2Te_5$, it could be significantly promoted by doping. For example, PCRAM cell based on Sb_2Te-11 at.% Si doping could be switched reversibly by using 1.1 V-100 ns SET pulse and 2.5 V- 50 ns RESET pulse as shown in Figure 8.

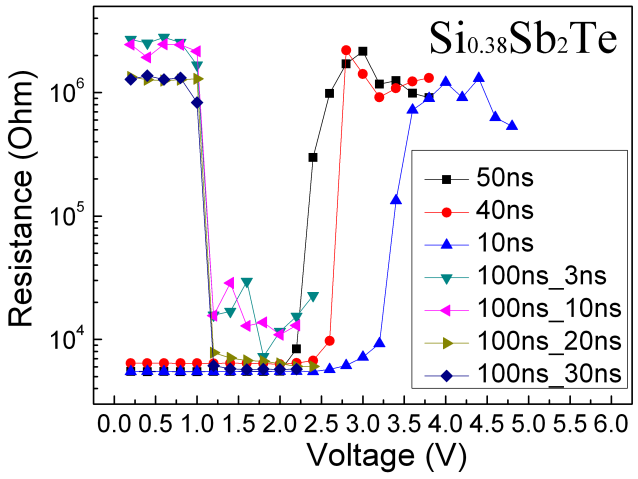

Figure 8: R-V curve for the $Si_{0.34}Sb_2Te$ based PCRAM cell.

4. CONCLUSION

New Sb-Te phase diagrams were developed by material library technique and far-field optical testing in this work. According to the phase diagrams achieved, Sb_xTe_{1-x} composition when x is in the range of 0.52 to 0.72 is promising for PCRAM applications. One typical composition, Sb_2Te, shows a good performance with high programming speed, high data retention, and medium programming power. PCRAM cells based on Sb_2Te with heating electrode size of 260 nm in diameter were fabricated and characterized. It could be switched between high resistance state and low resistance state by applying voltage of 1.9 and 4.3 V, respectively.

ACKNOWLEDGEMENT

The authors want to thank Dr. Qingfeng Liu and Prof. Qian Liu of Shanghai Institute of Ceramics (CAS) for the preparation of material chip samples. This work is supported by Chinese Academy of Sciences (083YQA1001), National Integrate Circuit Research Program of China (2009ZX02023-3), National Basic Research Program of China (2007CB935400 and 2006CB302700), and National High Technology Development Program of China (2008AA031402). T. Zhang would also like to thank the Alexander von Humboldt Foundation for a fellowship.

REFERENCES

[1] M. Wuttig and N. Yamada, Nat. Mater. **6** (2007) 824
[2]M. H. R. Lankhorst, B. W. S. M. M. Ketelaars, and R. A. M. Wolters, Nat. Mater. **4** (2005) 347
[3]B. Liu, Z. T. Song, S. L. Feng, and B. Chen, Microelectron. Eng. **82** (2005) 168
[4]M. H. R. Lankhorst, L. van Pieterson, M. van Schnijndel, B. A. J. Jacobs, and J. C. N. Rijpers, Jpn. J. Appl. Phys. **42** (2003) 863
[5]L. van Pieterson, M. H. R. Lankhorst, M. van Schnijndel, A. E. T. Kuiper, and J. H. J. Roosen, J. Appl. Phys. 97 (2005) 083520
[6]T. B. Massalski, Binary Alloy Phase Diagrams, 2nd edition, Vol. 3 (ASM International, 1990), p. 3308
[7]G. Ghosh, J. Phase Equilibria, **15** (1994) 349
[8]T. Zhang, Z. T. Song, F. Rao, G. M. Feng, B. Liu, S. L. Feng, and B. Chen, Jpn. J. Appl. Phys. **46** (2007) L247

Biographies

Dr. Ting Zhang was born in 1982. He received his B.S. degree and Ph. D. degree in Electrical Engineering in 2003 and 2008, respectively, from Xi'an Jiaotong University and Chinese Academy of Sciences. Since 2008, he works in Shanghai Institute of Microsystem (CAS) as an assistant professor. He is now also a postdoctoral research fellow in Institute of Physics, RWTH Aachen University.